Palm Line Extraction and Matching for Personal Authentication

Xiangqian Wu, *Member, IEEE*, David Zhang, *Senior Member, IEEE*, and Kuanquan Wang, *Member, IEEE*

***Abstract*—The palm print is a new and emerging biometric feature for personal recognition. The stable line features or "palm lines," which are comprised of principal lines and wrinkles, can be used to clearly describe a palm print and can be extracted in low-resolution images. This paper presents a novel approach to palm line extraction and matching for use in personal authentication. To extract palm lines, a set of directional line detectors is devised, and then these detectors are used to extract these lines in different directions. To avoid losing the details of the palm line structure, these irregular lines are represented using their chain code. To match palm lines, a matching score is defined between two palm prints according to the points of their palm lines. The experimental results show that the proposed approach can effectively discriminate between palm prints even when the palm prints are dirty. The storage and speed of the proposed approach can satisfy the requirements of a real-time biometric system.**

***Index Terms*—Biometrics, chain code, line extraction, line matching, palm line, palm print recognition.**

I. Introduction

COMPUTER-AIDED personal recognition is becoming increasingly important in our information-based society, and within this field biometrics is one of the most important and reliable methods [1], [2]. The most widely used biometric feature is the fingerprint [3], [4] and the most reliable feature is the iris [1], [5], [6]. However, it is very difficult to extract small unique features (known as minutiae) from unclear fingerprints [3], [4] and iris input devices are very expensive. Other biometric features, such as the face [7], [8] and the voice [9], [10], are as yet not sufficiently accurate. Compared with all of these, the palm print, a relatively new biometric feature, has several advantages [11]. Palm prints contain more information than fingerprints, so they are more distinctive. Palm print capture devices are much cheaper than iris devices. Further, palm prints contain additional distinctive features such as principal lines and wrinkles, which can be extracted from low-resolution images. By combining all the features of palms, such as palm geometry, ridge and valley features, and principal lines and wrinkles, it is possible to build a highly accurate biometrics system.

Much research has focused on offline palm print recognition [12]. An offline palm print image is obtained as follows: 1) ink a palm; 2) press the inked palm onto a white paper; 3) scan the image from the paper into a computer. Obviously, this method is time consuming and impractical. A further severe limitation from an applications point of view is that offline palm print recognition systems cannot work in real time. In order to overcome these problems, some researchers have turned to online palm print recognition and have obtained some good results. Zhang *et al.* [13] used two-dimensional (2-D) Gabor filters to extract texture features from low-resolution palm print images captured using a charge-coupled device (CCD) camera and employed these features to implement a highly accurate online palm print recognition system. You *et al.* [14] hierarchically coded the palm prints with multiple features for personal identification in large databases. Zhang and Zhang [15] characterized palm prints by wavelet signature via directional context modeling. Han *et al.* [16] used Sobel and morphological operations to extract line-like features from palm print images obtained using a scanner. Similarly, for verification, Kumar *et al.* [17] used other directional masks to extract line-like features from the palm prints captured using a digital camera. None of these palm print recognition methods, however, explicitly extracted the palm lines from the online palm prints and none of them made use of palm line structural features. Yet, palm line structural features are a natural choice for use in palm print recognition in that they can describe a palm print clearly and are robust against illumination and noises. In this paper, we devise a set of directional line detectors according to the palm lines' properties and then use them to detect the palm lines in different directions. To avoid losing the details of the palm line structure, these irregular lines are represented by their chain code. To match palm prints, we compute a matching score between two palm prints according to the points of their palm lines.

When palm prints are captured, the position, direction, and amount of stretching of a palm may vary so that even palm prints from the same palm may have little rotation and translation. Furthermore, palms differ in size. Hence, palm print images should be orientated and normalized before feature extraction and matching. Our CCD-based palm print capture device [13] is fitted with some pegs to limit the palm's stretching, translation, and rotation. These pegs separate the fingers, forming holes, one between the forefinger and the middle finger, and the other between the ring finger and the little finger.

Manuscript received February 9, 2004; revised November 2, 2004. This work was supported in part by the UGC/CRC fund from the HK SAR Government, the central fund from the Hong Kong Polytechnic University, and the Natural Science Foundation of China fund under Contracts 60441005 and 60332010. This paper was recommended by Associated Editor M. S. Obaidat.

X. Wu and K. Wang are with the School of Computer Science and Technology, Harbin Institute of Technology, Harbin 150001, China (e-mail: xqwu@hit.edu.cn; wangkq@hit.edu.cn).

D. Zhang is with the Biometrics Research Centre, Department of Computing, Hong Kong Polytechnic University, Kowloon, Hong Kong (e-mail: csdzhang@comp.polyu.edu.hk).

Digital Object Identifier 10.1109/TSMCA.2006.871797

In this paper, we use the preprocessing technique described in [13] to align the palm prints. This technique computes the tangent of these two holes and uses this information to align the palm print. The central part of the image, which is 128×128, is then cropped to represent the whole palm print. Such preprocessing greatly reduces the translation and rotation of the palm prints captured from the same palms.

The rest of this paper is organized as follows. Section II discusses palm line extraction and representation. Section III presents palm print matching. Section IV contains some experimental results and analyses. In Section V, we provide the conclusion.

II. Palm Line Extraction and Representation

Palm lines, including principal lines and wrinkles, are a kind of roof edge. A roof edge is generally defined as a discontinuity in the first-order derivative of a gray-level profile [18]. In other words, the positions of the roof edge points are the zero-cross points of their first-order derivative. The magnitude of the edge points' second derivative can reflect the strength of these edge points [19]. These properties can be used to detect palm lines, but the directions of palm lines are arbitrary, and it is very difficult to obtain their directions directly from noisy images, so in this section we discuss the detection of palm lines in different directions and we call lines that are detected in θ direction θ-directional lines and the detectors that detect θ-directional lines as θ-directional line detectors.

Suppose that $I(x, y)$ denotes an image. We devise the horizontal line detector (0°-directional line detector). To improve the connection and smoothness of the lines, the image is smoothed along the line direction (horizontal direction) using a one-dimensional (1-D) Gaussian function G_{σ_s} with variance σ_s, i.e.,

$$I_s = I * G_{\sigma_s} \tag{1}$$

where "$*$" is the convolve operation, which is used to implement linear filtering of the image [20].

The first- and second-order derivatives in the vertical direction can be computed by convolving the smoothed image with the first-order (G'_{σ_d}) and second-order (G''_{σ_d}) derivatives of a 1-D Gaussian function G_{σ_d} with variance σ_d in this direction, i.e.,

$$\begin{aligned} I'_{0^\circ} &= I_s * (G'_{\sigma_d})^T = (I * G_{\sigma_s}) * (G'_{\sigma_d})^T \\ &= I * \left(G_{\sigma_s} * (G'_{\sigma_d})^T\right) = I * \mathbf{H^1_{0^\circ}} \end{aligned} \tag{2}$$

$$\begin{aligned} I''_{0^\circ} &= I_s * (G''_{\sigma_d})^T = (I * G_{\sigma_s}) * (G''_{\sigma_d})^T \\ &= I * \left(G_{\sigma_s} * (G''_{\sigma_d})^T\right) = I * \mathbf{H^2_{0^\circ}} \end{aligned} \tag{3}$$

where "T" is the transpose operation, "$*$" is the convolve operation, and $\mathbf{H^1_{0^\circ}} = G_{\sigma_s} * (G'_{\sigma_d})^T$ and $\mathbf{H^2_{0^\circ}} = G_{\sigma_s} * (G''_{\sigma_d})^T$ are called the horizontal line detectors (0°-directional line detectors).

The horizontal lines can be obtained by looking for the zero-cross points of I'_{0° in the vertical direction and their strengths are the values of the corresponding points in I''_{0°, i.e.,

$$L^1_{0^\circ}(x, y) = \begin{cases} I''_{0^\circ}(x, y), & \text{if } I'_{0^\circ}(x, y) = 0 \text{ or} \\ & \quad I'_{0^\circ}(x, y) \times I'_{0^\circ}(x, y+1) < 0 \\ 0, & \text{otherwise.} \end{cases} \tag{4}$$

Furthermore, we can determine the type of a roof edge (line), i.e., valley or peak, from the sign of the values in $L^1_{0^\circ}(x, y)$: plus signs represent valleys, whereas minus signs represent peaks. Since all palm lines are valleys, the minus values in $L^1_{0^\circ}(x, y)$ should be discarded, i.e.,

$$L^2_{0^\circ}(x, y) = \begin{cases} L^1_{0^\circ}(x, y), & \text{if } L^1_{0^\circ}(x, y) > 0 \\ 0, & \text{otherwise.} \end{cases} \tag{5}$$

Palm lines are much thicker than ridges. For that reason, one or more thresholds can be used to remove ridges from $L^2_{0^\circ}$ and obtain a binary image L_{0°, which is called the 0°-directional line image.

The θ-directional line detectors $\mathbf{H^1_\theta}$ and $\mathbf{H^2_\theta}$ can be obtained by rotating $\mathbf{H^1_{0^\circ}}$ and $\mathbf{H^2_{0^\circ}}$ with angle θ. The first- and second-order derivatives in the direction $\theta + 90^\circ$ (denoted as I'_θ and I''_θ) can be obtained by convolving the image with $\mathbf{H^1_\theta}$ and $\mathbf{H^2_\theta}$. And the line points can be obtained by looking for the zero-cross points of I'_θ in the $\theta + 90^\circ$ direction. After discarding the peak roof edges and thresholding, we can obtain the binary θ-directional line image L_θ.

Finally, all of the directional line images are combined to obtain a line image, denoted as L, as

$$L(i, j) = \bigvee_{\text{all } \theta} L_\theta(i, j) \tag{6}$$

where "$\vee$" is a logical "OR" operation. After conducting the closing and thinning operations, we obtain the resultant palm line image. Fig. 1 shows the process of palm line extraction: (a) is an original palm print image; (b) to (e) are the 0°-, 45°-, 90°-, and 135°-directional line images, respectively; (f) is the resultant palm line image; and (g) is the original palm print overlapped with the extracted palm lines.

There are two parameters in these directional line detectors, namely, 1) σ_s and 2) σ_d. σ_s controls the connection and smoothness of the lines, and σ_d controls the width of the lines that can be detected. A small σ_s results in the poor connection and the poor smoothness of the detected lines, while a large σ_s results in the loss of some short lines and of line segments with large curvatures. Thin roof edges cannot be extracted when σ_d is large. Therefore, σ_s and σ_d are database dependent. In general, palm lines are long, narrow, and somewhat straight, thus for palm line extraction σ_s should be large while σ_d should be small. According to these properties of σ_s and σ_d, in this paper, we chose tens of typical palm prints from our database to manually tune the values of these parameters in numerous experiments (evaluating the experimental results visually) and obtained the parameters suitable for palm line extraction: $\sigma_s = 1.8$ and $\sigma_d = 0.5$. Using these values, it is possible to extract the majority of the palm lines from various

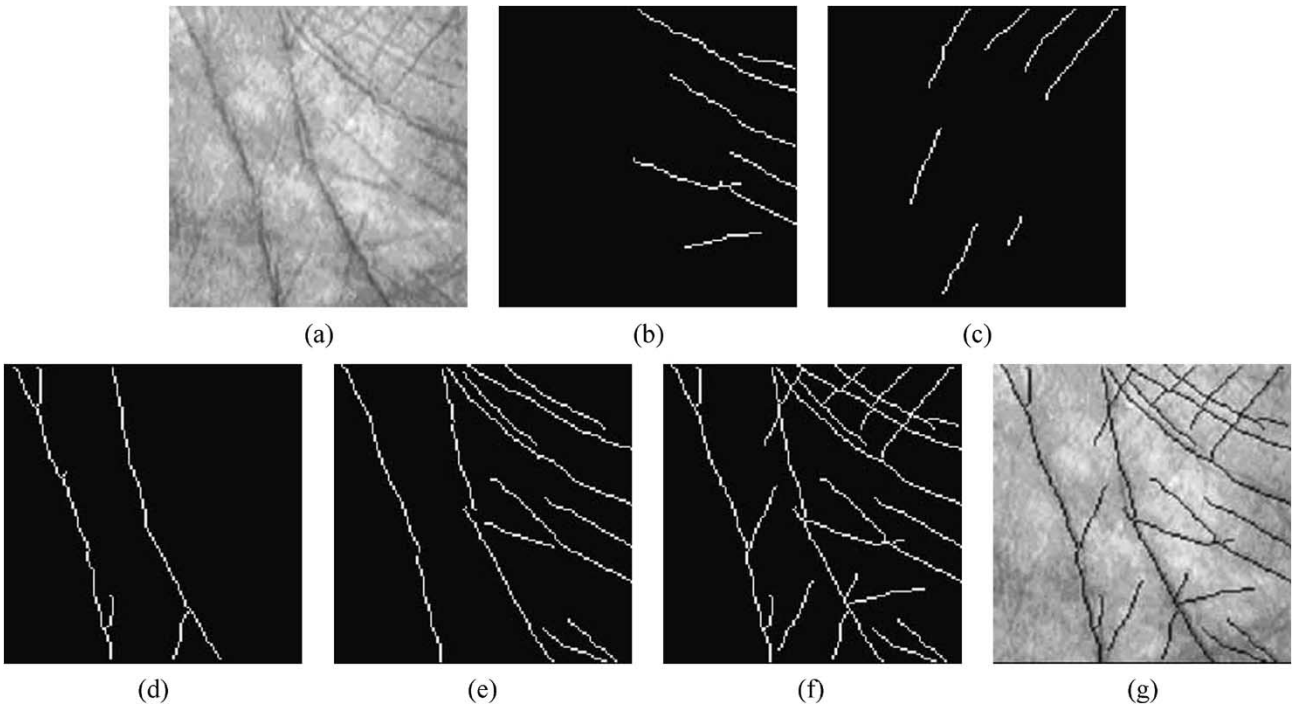

Fig. 1. Process of palm line extraction. (a) Original image. (b) 0°-directional lines. (c) 45°-directional lines. (d) 90°-directional lines. (e) 135°-directional lines. (f) Resultant palm lines. (g) Original palm print overlapped with the extracted palm lines.

palm prints. Nevertheless, it is impossible to use the same σ_s and σ_d to extract all of the lines from various palm prints. There are many factors that can affect the result of palm line extraction, such as the quality of the images, the value of the parameters, and the complexity of the palm line structures. On some palms with complex line structures, some lines may not be extracted. However, using these values of σ_s and σ_d does not greatly affect the recognition accuracy since majority of the palm lines have been extracted. The values of the components in matrices $\mathbf{H_{0^\circ}^1}$ and $\mathbf{H_{0^\circ}^2}$ (the contents of the matrices), which are computed by using (2) and (3), become smaller with the extension of their distance from the matrices' centers. Because the components with small values little affect the results of line extraction, there was no need to use all of the components to extract palm lines. Additional experimental results show that $\mathbf{H_{0^\circ}^1}$ and $\mathbf{H_{0^\circ}^2}$ with size 5 by 9 suffice for palm line extraction and the use of larger sizes does not greatly improve the results. Based on these experiments, $\mathbf{H_{0^\circ}^1}$ and $\mathbf{H_{0^\circ}^2}$, which are suitable for palm line extraction, can be computed as that shown in (7) and (8) at the bottom of the page.

Fig. 2 shows some examples of the extracted palm lines in which (a) is the original palm print images, (b) is the extracted palm lines, and (c) is the palm print images overlapped with the extracted palm lines. In these examples, 0°-, 45°-, 90°- and 135°-directional line detectors are used for palm line extraction.

Because palm lines have irregular shapes, it is very difficult to represent them in a mathematical form. One efficient method for representing irregular lines is the chain code [20]. We define the direction code of a pixel on a line as an integer between 0 and 7 according to the next line pixel it is pointing to [see Fig. 3(a)]. A chain code is a pixel-by-pixel direction code of a line. The chain code of a palm line can be obtained by line tracing: 1) obtain the coordinates of its beginning point; 2) trace

$$\mathbf{H_{0^\circ}^1} = \begin{bmatrix} 0.0009 & 0.0027 & 0.0058 & 0.0092 & 0.0107 & 0.0092 & 0.0058 & 0.0027 & 0.0009 \\ 0.0065 & 0.0191 & 0.0412 & 0.0655 & 0.0764 & 0.0655 & 0.0412 & 0.0191 & 0.0065 \\ 0.0000 & 0.0000 & 0.0000 & 0.0000 & 0.0000 & 0.0000 & 0.0000 & 0.0000 & 0.0000 \\ -0.0065 & -0.0191 & -0.0412 & -0.0655 & -0.0764 & -0.0655 & -0.0412 & -0.0191 & -0.0065 \\ -0.0009 & -0.0027 & -0.0058 & -0.0092 & -0.0107 & -0.0092 & -0.0058 & -0.0027 & -0.0009 \end{bmatrix} \tag{7}$$

$$\mathbf{H_{0^\circ}^2} = \begin{bmatrix} 0.0156 & 0.0211 & 0.0309 & 0.0416 & 0.0464 & 0.0416 & 0.0309 & 0.0211 & 0.0156 \\ 0.0257 & 0.0510 & 0.0954 & 0.1441 & 0.1660 & 0.1441 & 0.0954 & 0.0510 & 0.0257 \\ -0.0298 & -0.1125 & -0.2582 & -0.4178 & -0.4896 & -0.4178 & -0.2582 & -0.1125 & -0.0298 \\ 0.0257 & 0.0510 & 0.0954 & 0.1441 & 0.1660 & 0.1441 & 0.0954 & 0.0510 & 0.0257 \\ 0.0156 & 0.0211 & 0.0309 & 0.0416 & 0.0464 & 0.0416 & 0.0309 & 0.0211 & 0.0156 \end{bmatrix} \tag{8}$$

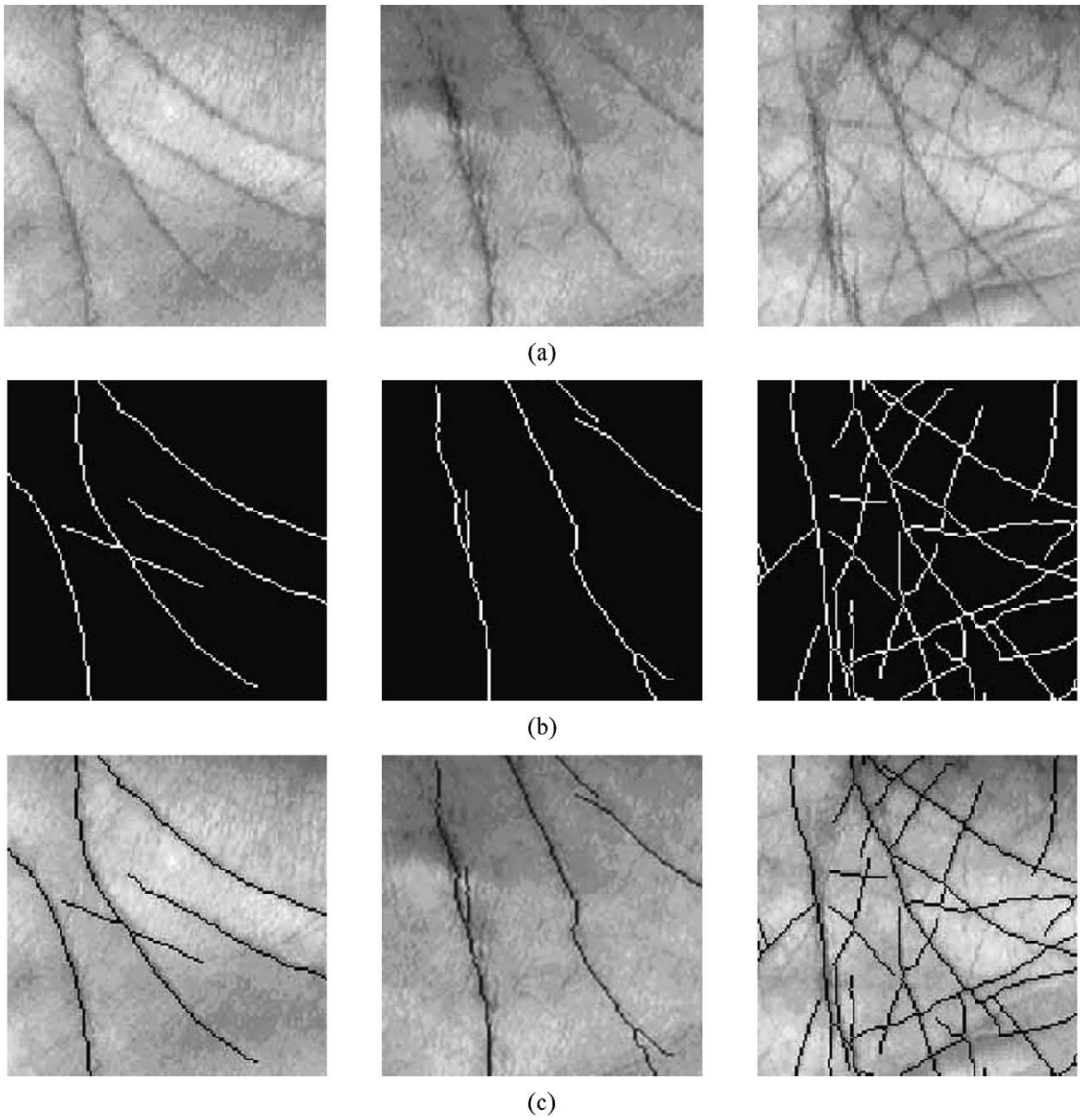

Fig. 2. Some results of palm line extraction. (a) Original images. (b) Extracted palm lines. (c) Palm print images overlapped with the extracted palm lines.

this line from the beginning point and obtain the direction code sequence $\{c_1, c_2, \ldots\}$. In the line tracing process, if there are branches, we choose one at random and continue the tracing along that branch. This representation allows the palm lines to be easily and accurately restored. Fig. 3(b) and (c) provides an example of the chain code of an irregular line.

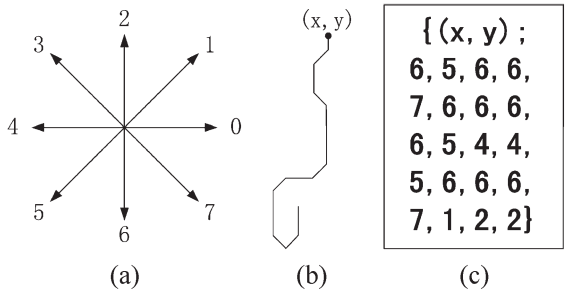

Fig. 3. Chain code. (a) Definition of the direction code. (b) Line. (c) Chain code of the line in (b).

III. Palm Line Matching

Template matching is a popular technique in pattern recognition for comparing a prestored template with a pattern. In this paper, the palm print templates are their chain codes and the palm line image of an input palm print is compared with the templates. In this section, we define the similarity measurement of a palm print template and a palm line image.

Let L denote a palm line image and C denote a template represented by chain codes. The most natural way to match L against C is to compute the proportion of the line points that are in the same position in L and in the palm line image, L_C, restored from C. However, because of the existence of noise, the line points of the same lines may be not superposed on the palm prints captured from the same palm at a different time. Fortunately, the point shift that results from the noise should be

small. Therefore, we can first dilate L to get L_D and then count the overlapping points between L_D and L_C. These overlapping points are regarded as the matched points of L and L_C. The matching score between L and C is defined as the proportion of matched points to the total line points in L and L_C, i.e.,

$$S(L,C) = \frac{2}{M_L + M_C} \sum_{i=1}^{M} \sum_{j=1}^{N} [L_D(i,j) \wedge L_C(i,j)] \quad (9)$$

where "$\wedge$" is the logical "AND" operation, $M \times N$ is the size of L, and M_C and M_L are the number of nonzero points in L_C and L, respectively.

From (9), we have to scan the whole image to compute the matching score, which is time consuming. In fact, (9) is equivalent to

$$S(L,C) = \frac{2}{M_L + M_C} \sum_{i=1}^{M_C} L_D(x_i, y_i) \quad (10)$$

where L_D is the dilated image of L, M_C is the total number of line points restored from C and $(x_i, y_i)(i = 1, \ldots, M_C)$ are their coordinates, and M_L is the number of line points in L. Obviously, the computational complexity of (10) is much less than that of (9). Moreover, if we use (10) to compute the matching score, instead of restoring the palm line image, L_C, from C, we only need to restore the coordinates of the line points.

It should be noted that $S(L,C)$ is not symmetrical, that is, $S(L_1, C_2)$ may not equal $S(L_2, C_1)$, where L_1 and L_2 are two palm line images and C_1 and C_2 are their chain codes, respectively. However, in general, the difference between $S(L_1, C_2)$ and $S(L_2, C_1)$ is small. We have tested the difference using 28 914 210 pairs of palm print images. The average difference is about 0.0095 and the maximum difference is about 0.078.

Obviously, $S(L,C)$ is between 0 and 1, and the larger the matching score the greater the similarity between L and C. The matching score of a perfect match is 1. Because of imperfect preprocessing, there may still be little rotation and translation between the palm prints captured from the same palm at different times. To remove the rotation effect, we rotate L a few degrees and then merge all the rotated images by using logical "OR" binary image L_M. After that, L_M is dilated to obtain L_{MD}, and to compute the matching score, we replace L_D with L_{MD} in (10). To overcome the translation problem, we vertically and horizontally translate C a few points, and then, at each translated position, compute the matching score between the translated C and L_{MD}. Finally, the final matching score is taken to be the maximum matching score of all the translated positions. The ranges of the palm print rotation and translation are dependent on the database. Fig. 4 shows the entire process of palm line matching. In this figure, the input palm line image and Template 1 are from one palm and Template 2 is from another palm. The matching scores between the input sample and Template 1 and between the input sample and Template 2 are 0.9806 and 0.1771, respectively. The matching scores between the palm prints in Fig. 2 are listed in Table I.

IV. Experimental Results and Analysis

A. Palm Print Databases and Experimental Conditions

For our experiments, we established three palm print databases, namely, DB1, DB2, and DB3. The large database DB1, which contains 7605 palm prints collected from 392 different palms, was established for palm print matching and recognition tests. These palm prints were taken from people of different ages and both sexes and were captured twice, at an interval of around two months, each time taking about ten images from each palm. Therefore, DB1 contains about 20 images of each palm. The images in DB1 are of two different sizes, 384 $\times$ 284 and 768 $\times$ 568. Fig. 5 shows some samples from DB1. The smaller databases DB2 and DB3 contain 400 palm prints from 40 different palms. These two smaller databases were established as follows. First, from the 40 palms, we took 400 images (ten images per palm) to build DB2. These palms were clean but were then made dirty by being rubbed with common garden soil. These soiled hands were then used to obtain another 400 images (again ten images per palm) to build DB3. The mean and standard deviation of all point values of all samples from each palm in DB2, DB3, and their differences, which are listed in Table II, reflect just how dirty the soiled palms were. As Table II shows, the palms that were used to construct DB3 were made dirty to different degrees. DB2 and DB3 were used to investigate the effect of the dirty palms on the performance of the proposed approach. All of the images in DB2 and DB3 are 800 $\times$ 571. Fig. 6 shows some palm prints from DB2 and DB3. In our experiments, all images were resized to 384 $\times$ 284, and, using the preprocessing technique described in [13], the central 128 $\times$ 128 part of the image was cropped to represent the whole palm print. The capture device used to collect the palm prints can control the light condition, and we have given some instructions to the subjects for using this device when we collected their palm prints. Therefore, the qualities of the collected samples are good enough for successful cropping by the preprocessing technique.

Many other experiments with different directional line detectors have been carried out to test the proposed approach. The results showed that 0°-, 45°-, 90°-, and 135°-directional line detectors are sufficient for palm line extraction and the use of extra detectors does not greatly improve the results. Therefore, in this section, to extract palm lines, we used these four directional line detectors, which were computed according to $\mathbf{H_0^1}_\circ$ and $\mathbf{H_0^2}_\circ$ in (7) and (8). The hysteresis thresholding method [21] was used. This method employs dual thresholds T_H and T_L $(T_H > T_L)$. The points whose values exceed T_H constitute strong lines and the points whose values are between T_L and T_H constitute weak lines. The strong lines and those weak lines connecting with some strong ones are kept as the final palm lines. In the experiments, T_L was chosen as the minimum value of the nonzero points of all L_θ^1, and T_H was chosen automatically using Otsu's method [22], which splits the histogram of the nonzero points of all L_θ^1 such that the variance of each pixel group is minimized. In the palm line matching process, the ranges of the rotation were -2° to 2° (the step is 1°) and the ranges of vertical and horizontal translations were -5 to 5 pixels (the step is 1 pixel).

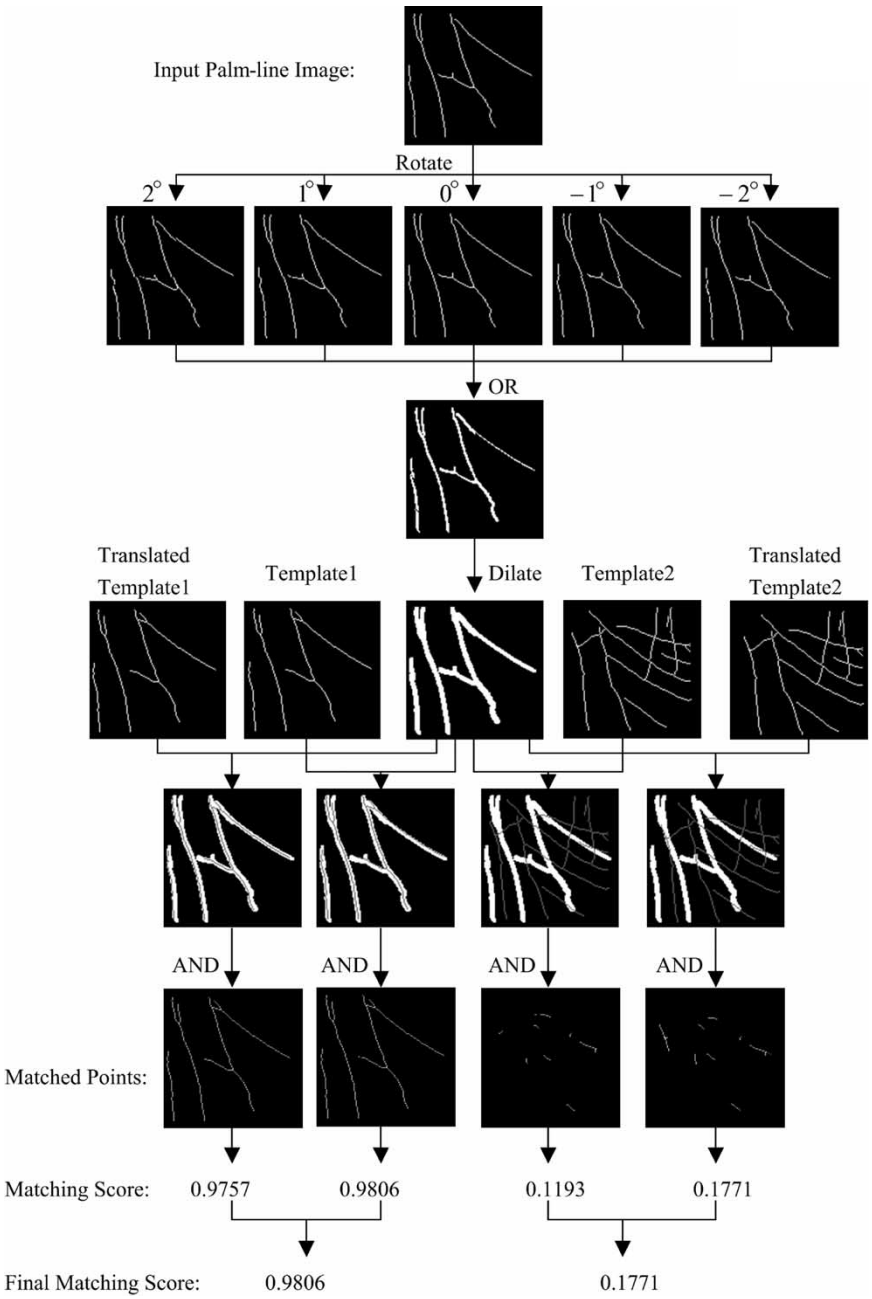

Fig. 4. Process of palm line matching.

TABLE I
MATCHING SCORES BETWEEN THE PALM PRINTS IN FIG. 2

Column	Left	Middle	Right
Left	1	0.1816	0.2046
Middle	0.1742	1	0.1902
Right	0.1840	0.1866	1

B. Palm Print Matching

To test the performance of the proposed approach in palm print matching, each sample in DB1 is matched against the other palm prints in the same database. The matching between palm prints, which were captured from the same palm, is defined as a genuine matching. Otherwise, the matching is defined as an impostor matching. A total of 57 828 420 (7605 × 7604) matchings have been performed, in which 141 004 matchings are genuine matchings. None of the matching scores is 1. The failure to enroll rate is zero. Fig. 7 shows the distributions of the genuine and impostor matching scores. It is shown that there are two distinct peaks in the distributions of the matching scores. One peak (located around 0.80) corresponds to the genuine matching scores while the other peak (located around 0.23) corresponds to the impostor matching scores. These two peaks are widely separated and the distribution curve of the genuine matching scores intersects very little with that of impostor matching scores. Therefore, the proposed approach can very effectively discriminate between palm prints.

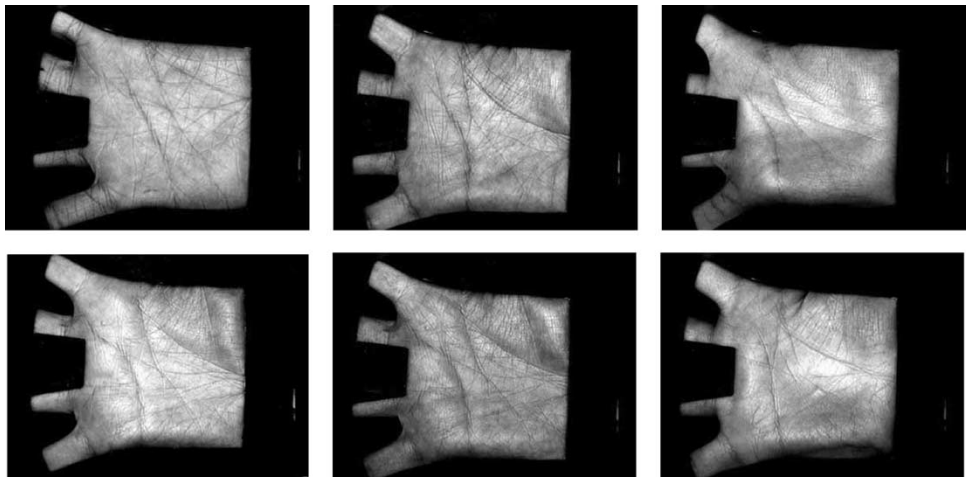

Fig. 5. Typical palm prints from DB1.

TABLE II
MEAN AND STANDARD DEVIATION OF ALL POINT VALUES OF ALL SAMPLES FROM EACH PALM IN DB2, DB3, AND THEIR DIFFERENCES

Palm	Mean			Standard Deviation		
No.	DB2	DB3	Diff.	DB2	DB3	Diff.
1	152.6	149.2	3.4	37.1	32.9	4.3
2	154.9	151.3	3.6	36.7	37.4	-0.7
3	156.4	132.1	24.3	43.8	52.6	-8.9
4	155.6	138.3	17.3	40.2	53.3	-13.0
5	150.5	141.4	9.1	40.3	35.1	5.2
6	156.2	137.3	18.9	40.6	49.3	-8.7
7	149.8	137.0	12.9	39.4	47.6	-8.2
8	152.7	143.6	9.1	40.8	35.4	5.4
9	157.0	148.7	8.3	40.8	34.0	6.8
10	156.4	142.9	13.5	40.9	42.3	-1.4
11	151.8	135.1	16.7	40.7	49.6	-8.8
12	155.5	137.7	17.8	37.4	46.9	-9.5
13	152.0	146.4	5.6	37.9	38.6	-0.7
14	149.7	134.2	15.5	38.6	46.6	-8.0
15	157.9	154.6	3.3	46.3	50.9	-4.6
16	154.4	146.4	8.0	43.6	39.6	3.9
17	150.9	146.9	4.0	42.6	39.9	2.6
18	154.1	146.1	8.0	42.7	43.4	-0.7
19	155.5	146.5	9.0	38.0	35.2	2.8
20	153.6	149.9	3.8	36.4	35.5	0.9
21	149.4	125.9	23.5	38.2	50.1	-11.9
22	154.1	140.1	13.9	36.8	48.3	-11.5
23	148.0	141.8	6.2	40.8	38.5	2.3
24	151.0	141.3	9.7	39.8	49.6	-9.9
25	154.9	141.9	13.1	41.6	49.1	-7.5
26	153.9	143.8	10.1	40.7	34.0	6.6
27	156.3	150.5	5.8	40.0	33.1	6.9
28	156.8	150.8	6.0	42.0	40.6	1.4
29	154.8	132.3	22.5	42.0	51.0	-9.0
30	154.0	143.0	11.0	39.4	49.3	-9.9
31	151.8	141.4	10.4	37.6	44.5	-6.9
32	150.6	136.7	13.9	39.1	56.9	-17.8
33	158.2	152.6	5.6	45.2	39.7	5.5
34	152.5	145.8	6.7	41.3	34.3	7.0
35	150.1	147.5	2.6	38.8	35.7	3.1
36	155.4	148.6	3.5	41.2	43.3	-2.2
37	151.1	145.2	5.9	35.5	29.2	6.3
38	153.6	144.4	9.1	40.5	48.3	-7.8
39	149.8	136.5	13.3	37.7	35.4	2.3
40	150.5	142.1	8.5	47.0	56.5	-9.5

C. Palm Print Verification

Palm print verification, also called one-to-one matching, involves answering the question "whether this person is who he or she claims to be" by examining his or her palm print. In palm print verification, a user indicates his or her identity and thus the input palm print is matched only against his or her stored template. To determine the accuracy of the verification, each sample in DB1 is matched against the other palm prints in the same database. If the matching score exceeds a given threshold, the input palm print is accepted. If not, it is rejected. The performance of a verification method is often measured by the false accept rate (FAR) and false reject rate (FRR). While it is ideal that these two rates be as low as possible, they cannot be lowered at the same time. So, depending on the application, it is necessary to make a tradeoff: for high security systems, such as some military systems, where security is the primary criterion, we should reduce FAR, while for low security systems, such as some civil systems, where ease-of-use is also important, we should reduce FRR. To test the performance of a verification method with respect to the FAR and FRR tradeoff, we usually plot the so-called receiver operating characteristic (ROC) curve, which plots the pairs (FAR, FRR) with different thresholds [4]. Fig. 8 shows the ROC curves of the proposed approach, of the 2-D Gabor algorithm [13], and of the Sobel method [16], which were implemented in DB1. The proposed approach's equal error rate (EER), where FAR equals FRR, is about 0.4%, while the EERs of the 2-D Gabor algorithm and the Sobel method are about 0.6% and 5.0%. According to this figure, the performances of the proposed approach and the 2-D Gabor algorithm are much better than that of the Sobel method. For further analysis, the ROC curves of the proposed approach and the 2-D Gabor algorithm are replotted in Fig. 9. From this figure, the proposed approach has a smaller FAR except when FRR exceeds 0.91%. This means that the 2-D Gabor algorithm is more suitable for some high security systems while the proposed approach is more suitable for the medium and low security systems.

D. Palm Print Identification

Palm print identification, also called one-to-many matching, seeks to answer the question "who is this person?" by examining his or her palm print. The input palm print is first

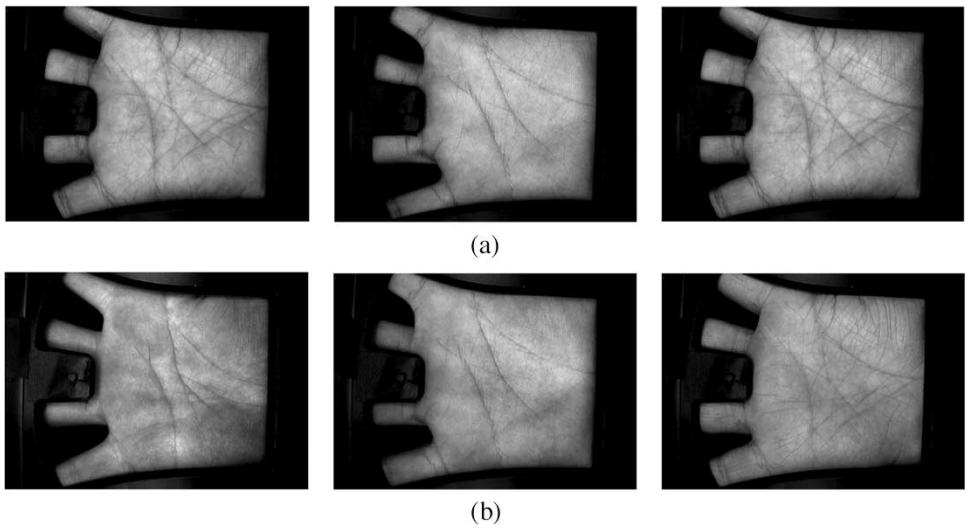

Fig. 6. Some palm prints from DB2 and DB3. (a) Clean palm prints from DB2. (b) Dirty palm prints from DB3.

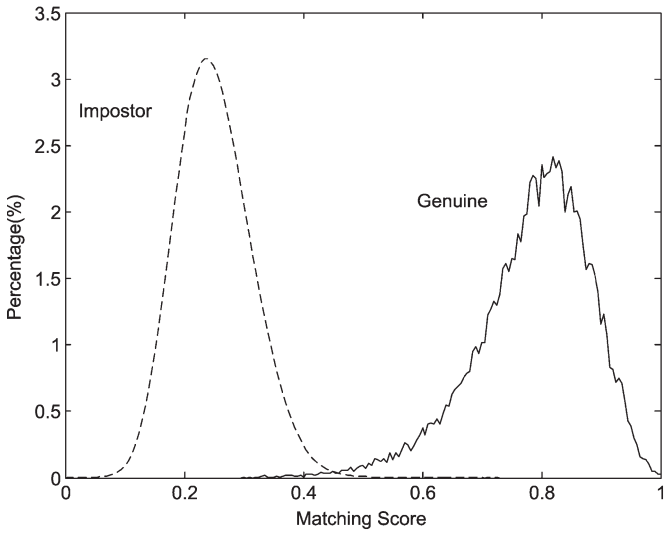

Fig. 7. Distribution of palm print matching scores.

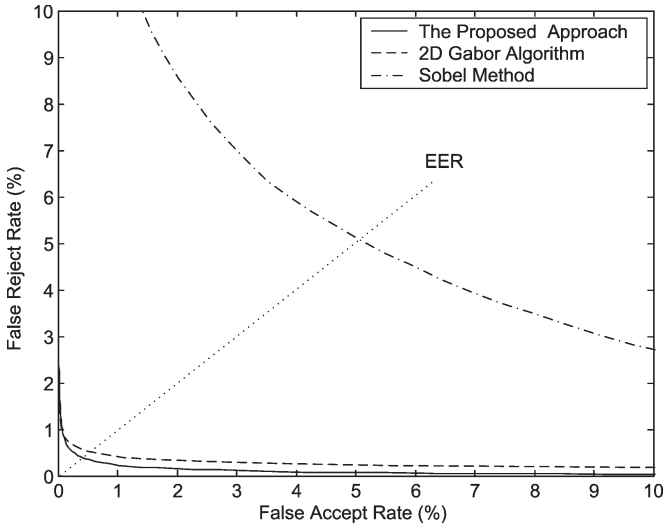

Fig. 8. ROC curves of the proposed approach, 2-D Gabor algorithm, and Sobel method in DB1.

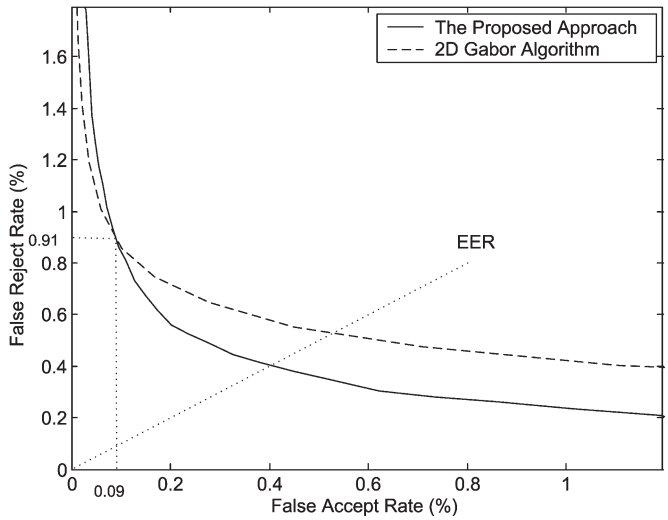

Fig. 9. Replotting ROC curves of the proposed approach and 2-D Gabor algorithm in DB1.

preprocessed, and then the palm line image is extracted from the preprocessed image. The palm line image is matched against each template in the template database and, finally, the label of the most similar template is obtained as the identification result. In our experiments, one palm print is randomly chosen as the template for each palm and the remaining palm prints are used as test samples, that is, there are 392 templates and 7213 test samples. The accuracies of the proposed approach, of the 2-D Gabor algorithm, and of the Sobel method are 97.81%, 96.63%, and 89.33%, respectively. Therefore, in palm print identification, the proposed approach outperforms the other two.

E. Dirty Palms: Their Effect Upon Performance

To investigate how dirty palms might affect the performance of the proposed approach, we matched each image in DB3, captured from dirty palms, against each image in DB2, captured

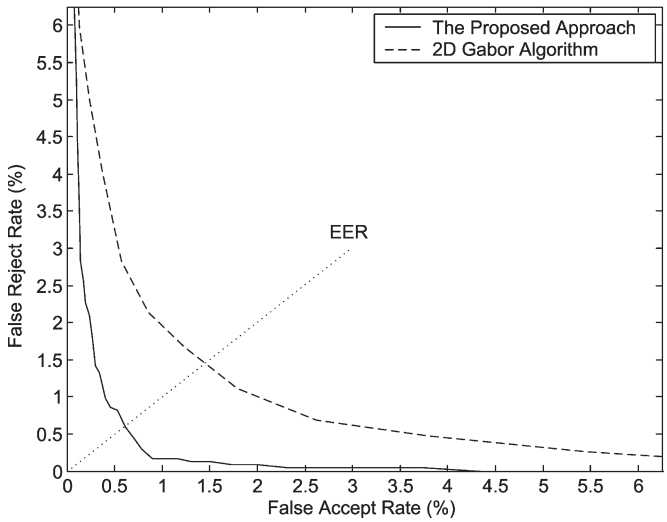

Fig. 10. ROC curves of proposed approach and 2-D Gabor algorithm in the case of dirty palm prints.

TABLE III
TYPICAL FAR, FRR, AND CORRESPONDING THRESHOLDS

The Proposed Approach			2D Gabor Algorithm		
Thresh	FAR	FRR	Thresh	FAR	FRR
0.38	2.31	0.04	0.35	0.01	16.92
0.38	1.99	0.09	0.36	0.01	13.80
0.39	1.72	0.09	0.36	0.02	11.62
0.39	1.51	0.13	0.37	0.04	9.57
0.40	1.31	0.13	0.37	0.07	7.48
0.40	1.16	0.17	0.38	0.13	5.98
0.41	1.02	0.17	0.38	0.24	5.00
0.41	0.90	0.17	0.39	0.37	4.02
0.42	0.79	0.30	0.39	0.57	2.82
0.42	0.70	0.43	0.40	0.85	2.14
0.43	0.61	0.60	0.40	1.24	1.67
0.43	0.53	0.81	0.41	1.79	1.11
0.44	0.46	0.85	0.41	2.62	0.68
0.44	0.40	0.98	0.42	3.80	0.47
0.45	0.34	1.32	0.42	5.46	0.26
0.45	0.30	1.41	0.43	7.62	0.09
0.46	0.27	1.79	0.43	10.69	0.04
0.46	0.23	2.09	0.44	14.88	0.00
0.47	0.19	2.27	0.44	20.66	0.00
0.47	0.17	2.56	0.45	28.05	0.00
0.48	0.14	2.82	0.45	37.66	0.00

from clean palms. Because of the poor performance of the Sobel method in palm print recognition, we do not consider it in this subsection. Fig. 10 shows the ROC curves of the proposed approach and the 2-D Gabor algorithm [13], where their EERs are 0.61 and 1.45%, respectively, that is, the EER of our approach is 0.84% less than that of 2-D Gabor algorithm. Some typical FAR and FRR and the corresponding thresholds are listed in Table III. Fig. 10 shows that the whole ROC curve of the proposed approach is below the curve of the 2-D Gabor algorithm, which means that the proposed approach outperforms the 2-D Gabor algorithm. In other words, our approach is more robust to dirty palms than the 2-D Gabor algorithm. This is because texture features as extracted in the 2-D Gabor algorithm are more easily obscured by dirt than are line features of the type extracted using the proposed approach.

TABLE IV
SPEED OF THE PROPOSED APPROACH

Stage	Preprocessing	Palm-line Extraction	Palmprint Matching
Time (ms)	538	82	2.2

F. Storage Requirements

Storage requirements are very important in biometric systems. The proposed approach represents palm prints using their palm line chain codes. Each palm line is stored with the coordinates of one of its endpoints and its chain code. Supposing the length of a palm line is L points, the length of its chain code will be $(L-1)$. Since 3 bits are needed to store a direction code (0, 1,..., 7), $3 \times (L-1)$ bits are needed to represent the whole chain code. The coordinates of one endpoint of the palm line have two components and 1 B is needed to store each component. Therefore, a total of $[2 + 3 \times (L-1)/8]$ B are needed to store each palm line. The statistical results from DB1 show that the average number of the palm lines of a palm print is about 22 and the average length of a palm line is about 28 points. Consequently, the average storage requirement for a palm print is about $22 \times [2 + 3 \times (28-1)/8] \approx 267$ B. The maximum and minimum storage requirements in these palm prints are 762 and 62 B, respectively.

G. Speed

Speed is a key factor in an on-line biometric system. The proposed approach is implemented using Visual C++ on a personal computer with Intel Pentium III processor (500 MHz). Table IV lists the average time that is required for preprocessing, palm line extraction, and matching. The average response time is about 0.6 s for verification and about $(620 + 2.2 \times N)/1000$ s for identification (N is the number of the templates), which is fast enough for a real-time biometric system.

V. CONCLUSION

Palm lines are one of the most important features of palm prints. In this paper, we have proposed a novel approach to palm line extraction and matching for personal authentication. A set of directional line detectors has been devised for palm line extraction, by which palm lines can be extracted effectively. To preserve the details of the lines' structure, palm lines are represented by their chain code and then palm prints are matched by matching the points on their palm lines. The experimental results on a general database (DB1) demonstrate the power of the proposed approach. In palm print verification, the proposed approach and the 2-D Gabor algorithm perform much better than the Sobel method. Furthermore, the proposed approach is more powerful for palm print verification than the 2-D Gabor algorithm when FRR $< 0.91\%$, and the EER of our approach (0.4%) is 0.2% less than that of 2-D Gabor algorithm (0.6%). In palm print identification, the proposed approach also outperforms the 2-D Gabor algorithm and the Sobel method. Another experiment testing its robustness against dirty palms (DB2 and

DB3) confirms the advantage of our approach over the 2-D Gabor algorithm, where the EER of our approach is 0.84% less than that of 2-D Gabor algorithm. In addition, the average memory requirement for a palm print is only 267 B and the average processing time, including the preprocessing, palm line extraction, and matching is only 0.6 s, proving the practicality of our approach. In conclusion, the proposed approach can distinguish palm prints effectively and is a promising algorithm for establishing a real personal authentication system using palm print biometrics.

ACKNOWLEDGMENT

This work was supported by the Natural Science Foundation of China and the central fund from the Hong Kong Polytechnic University. The authors are most grateful for the constructive advice and comments from the anonymous reviewers.

REFERENCES

[1] D. Zhang, *Automated Biometrics—Technologies and Systems*. Boston, MA: Kluwer, 2000.
[2] A. Jain, R. Bolle, and S. Pankanti, *Biometrics: Personal Identification in Networked Society*. Boston, MA: Kluwer, 1999.
[3] A. Jain, L. Hong, and R. Bolle, "On-line fingerprint verification," *IEEE Trans. Pattern Anal. Mach. Intell.*, vol. 19, no. 4, pp. 302–313, Apr. 1997.
[4] D. Maio, D. Maltoni, R. Cappelli, J. L. Wayman, and A. Jain, "FVC2000: Fingerprint verification competition," *IEEE Trans. Pattern Anal. Mach. Intell.*, vol. 24, no. 3, pp. 402–412, Mar. 2002.
[5] R. Wildes, "Iris recognition: An emerging biometric technology," *Proc. IEEE*, vol. 85, no. 9, pp. 1348–1363, Sep. 1997.
[6] W. Boles and B. Boashash, "A human identification technique using images of the iris and wavelet transform," *IEEE Trans. Signal Process.*, vol. 46, no. 4, pp. 1185–1188, Apr. 1998.
[7] R. Brunelli and T. Poggio, "Face recognition: Features versus templates," *IEEE Trans. Pattern Anal. Mach. Intell.*, vol. 15, no. 10, pp. 1042–1052, Oct. 1993.
[8] Y. Gao and M. Leun, "Face recognition using line edge map," *IEEE Trans. Pattern Anal. Mach. Intell.*, vol. 24, no. 6, pp. 764–779, Jun. 2002.
[9] J. Campbell, Jr., "Speaker recognition: A tutorial," *Proc. IEEE*, vol. 85, no. 9, pp. 1437–1462, Sep. 1997.
[10] K. Chen, "Towards better making a decision in speaker verification," *Pattern Recognit.*, vol. 36, no. 2, pp. 329–346, Feb. 2003.
[11] A. Jain, A. Ross, and S. Prabhakar, "An introduction to biometric recognition," *IEEE Trans. Circuits Syst. Video Technol.*, vol. 14, no. 1, pp. 4–20, Jan. 2004.
[12] N. Duta, A. Jain, and K. Mardia, "Matching of palmprint," *Pattern Recognit. Lett.*, vol. 23, no. 4, pp. 477–485, 2001.
[13] D. Zhang, W. Kong, J. You, and M. Wong, "Online palmprint identification," *IEEE Trans. Pattern Anal. Mach. Intell.*, vol. 25, no. 9, pp. 1041-1050, Sep. 2003.
[14] J. You, W. K. Kong, D. Zhang, and K. H. Cheung, "On hierarchical palmprint coding with multiple features for personal identification in large databases," *IEEE Trans. Circuits Syst. Video Technol.*, vol. 14, no. 2, pp. 234–243, Feb. 2004.
[15] L. Zhang and D. Zhang, "Characterization of palmprints by wavelet signatures via directional context modeling," *IEEE Trans. Syst., Man, Cybern. B, Cybern.*, vol. 34, no. 3, pp. 1335–1347, Jun. 2004.
[16] C. Han, H. Chen, C. Lin, and K. Fan, "Personal authentication using palmprint features," *Pattern Recognit.*, vol. 36, no. 2, pp. 371–381, Feb. 2003.
[17] A. Kumar, D. Wong, H. Shen, and A. Jain, "Personal verification using palmprint and hand geometry biometric," in *Lecture Notes in Computer Science*, vol. 2688. Berlin, Germany: Springer-Verlag, 2003, pp. 668–678.
[18] R. Haralick, "Ridges and valleys on digital images," *Comput. Vis. Graph. Image Process.*, vol. 22, no. 1, pp. 28–38, Apr. 1983.
[19] K. Liang, T. Tjahjadi, and Y. Yang, "Roof edge detection using regularized cubic b-spline fitting," *Pattern Recognit.*, vol. 30, no. 5, pp. 719–728, May 1997.
[20] K. R. Castleman, *Digital Image Processing*. Englewood Cliffs, NJ: Prentice-Hall, 1996.
[21] J. Canny, "A computational approach to edge detection," *IEEE Trans. Pattern Anal. Mach. Intell.*, vol. PAMI-8, no. 6, pp. 679–698, Nov. 1986.
[22] J. R. Parker, *Algorithms for Image Processing and Computer Vision*. Hoboken, NJ: Wiley, 1997.

Xiangqian Wu (M'06) received the B.Sc., M.Sc., and Ph.D. degrees in computer science from the Harbin Institute of Technology (HIT), Harbin, China, in 1997, 1999, and 2004, respectively.

In 2000, 2002, 2003, and 2006, he was a Research Assistant at the Hong Kong Polytechnic University, Kowloon, Hong Kong. He is currently a Lecturer at the School of Computer Science and Technology, HIT. He has published about 30 papers in several international journals and conferences. His current research interests include pattern recognition, image analysis, biometrics, etc. He is a Principal Investigator of several research projects, including the projects of the Natural Science Foundation of China. He is a reviewer for the *International Journal of Image and Graphics* and the *Journal of Computer Science and Technology*.

Dr. Wu won the Excellent Paper Award in the Third International Conference on Wavelet Analysis and Its Application and (ICWAA 2004) in 2004 and the Excellent PHD Dissertation Award of HIT in 2005. He is a reviewer for the IEEE TRANSACTIONS ON PATTERN ANALYSIS AND MACHINE INTELLIGENCE and the IEEE TRANSACTIONS ON SYSTEMS, MAN, AND CYBERNETICS—PART A.

David Zhang (SM'95) graduated in computer science from Peking University, Beijing, China, in 1974, and received the M.Sc. and Ph.D. degrees in computer science from the Harbin Institute of Technology (HIT), Harbin, China, in 1982 and 1985, respectively, and the Ph.D. degree in electrical and computer engineering from the University of Waterloo, Waterloo, ON, Canada.

From 1986 to 1988, he was a Postdoctoral Fellow at Tsinghua University, Beijing, China, and then an Associate Professor at Academia Sinica, Beijing. He is currently a Chair Professor at the Hong Kong Polytechnic University, Kowloon, Hong Kong, where he is the Founding Director of the Biometrics Technology Centre (UGC/CRC) supported by the Hong Kong SAR Government. He also serves as an Adjunct Professor at Tsinghua University, Shanghai Jiao Tong University, Beihang University, HIT, and the University of Waterloo. He is the Founder and Editor-in-Chief of the *International Journal of Image and Graphics*, Book Editor of the Kluwer International Series on Biometrics, and an Associate Editor of more than ten international journals including *Pattern Recognition* and is the author of more than ten books.

Dr. Zhang is Program Chair of the International Conference on Biometrics Authentication (ICBA) and an Associate Editor for the IEEE TRANSACTIONS ON SYSTEMS, MAN, AND CYBERNETICS—PART A and PART C. He is a current Croucher Senior Research Fellow and Distinguished Speaker of the IEEE Computer Society.

Kuanquan Wang (M'01) received the B.E. and M.E. degrees in computer science from the Harbin Institute of Technology (HIT), Harbin, China, in 1985 and 1988, respectively, and the Ph.D. degree in computer science from Chongqing University, Chongqing, China, in 2001.

From 1988 to 1998, he was with the Department of Computer Science, Southwest Normal University, Chongqing, as a Tutor, Lecturer, and Associate Professor. Since 1998, he has been with the Biocomputing Research Center, HIT, as a Professor, Supervisor of Ph.D. candidates, and an Associate Director. From 2000 to 2001, he was a Visiting Scholar at the Hong Kong Polytechnic University, Kowloon, Hong Kong, supported by the Hong Kong Croucher Funding, and from 2003 to 2004 was a Research Fellow. He has published over 70 papers. His research interests include biometrics, image processing, and pattern recognition. He is an Editor for the *International Journal of Image and Graphics* and a reviewer of *Pattern Recognition*.

Dr. Wang is a reviewer for the IEEE TRANSACTIONS ON SYSTEMS, MAN, AND CYBERNETICS.